Journal of Alloys and Compounds 489 (2010) 667–673

Contents lists available at ScienceDirect

Journal of Alloys and Compounds

journal homepage: www.elsevier.com/locate/jallcom

Efficient electrochromic nickel oxide thin films by electrodeposition

A.C. Sonavane[a], A.I. Inamdar[a,b], P.S. Shinde[a], H.P. Deshmukh[c], R.S. Patil[a], P.S. Patil[a,*]

[a] Thin Film Materials Laboratory, Department of Physics, Shivaji University, Kolhapur - 416 004, Maharashtra, India
[b] Department of Semiconductor Science, Dongguk University, Seoul - 100-715, Republic of Korea
[c] Department of Physics, Y. M. College, Bharati Vidyapeeth, Erandwane, Pune, India

ARTICLE INFO

Article history:
Received 25 August 2009
Accepted 23 September 2009
Available online 27 September 2009

Keywords:
Nickel oxide thin films
Electrodeposition
Electrochemical quartz crystal microbalance (EQCM)
Electrochemical properties (CV CA)
Scanning electron microscopy
XRD
Optical properties

ABSTRACT

Nickel oxide (NiO) thin films were prepared by electrodeposition technique onto the fluorine doped tin oxide (FTO) coated glass substrates in one step deposition at 20, 30, 40 and 50 min deposition times respectively. The effect of film thickness (thereby microstructural changes) on their structural, morphological, optical and electrochromic properties was investigated. The mass change with potential and cyclic voltammogram was recorded in the range from +0.3 to −0.8 V versus Ag/AgCl. One step deposition of polycrystalline cubic phase NiO was confirmed from X-ray diffraction study. Optical absorption study revealed direct band gap energy of 3.2 eV. The optical transmittance of the film decreased with increase in film thickness. A uniform granular and porous morphology of the films deposited for 20 min was observed. The film becomes more compact and devoid of pores when deposition time was increased to 30 min. Thereafter severe cracks are observed. All the films exhibit anodic electrochromism in OH^- containing electrolyte (0.1 M KOH). The maximum coloration efficiency of 107 cm^2/C and electrochemical stability of up to 10^4 colour/bleach cycles were observed for the films deposited for 20 min (film thickness of 104 nm).

1. Introduction

Nickel oxide (NiO) is the most exhaustively investigated transition metal oxide exhibiting semiconducting properties. It offers promising candidature for many applications such as electrocatalysis or electrosynthesis [1,2], positive electrode in batteries [3], fuel cell [4], electrochromic devices with good electrochemical stability and cyclic durability [5–8], solar thermal absorber [9], catalyst for oxygen evolution [10] and photo electrolysis [11].

Many reports published on hydrated nickel oxide films lead to the conclusion that the film properties are strongly influenced by deposition techniques like thermal decomposition [12], RF sputtering [13], electron beam evaporation [14], dc magnetron sputtering [15], anodic electrodeposition [16,17], cathodic electrodeposition [18], chemical deposition [19], sol–gel technology [8,12] and spray pyrolysis technique [20]. Electrochromism in NiO thin films is rather complicated although it is generally accepted that the transition from a coloured to a bleached state is related to a charge-transfer process between Ni (II) and Ni (III) [21]. Certain oxides (viz. tungsten oxide) have high transparency in the bleached state, whereas nickel oxide has a residual brown tint in the bleached state which can be reduced using additives such as Mg, Al, Si,Zr, Nb or Ta [22–25]. Of all the physical and chemical deposition techniques, electrodeposition is of particular interest due to low-cost, environmental friendly process, and feasibility of room temperature growth on large area [26]. Cathodically electrodeposited films showed some improvement in adherence and little improvement in the charge capacity upon thermal treatment [27]. But, electrodeposited films exhibit ageing after a few cycles [27–29]. Better transmittance modulation and durability were found with addition of Ce and La by cathodic electrodeposition [28,29]. A new trend in device construction is to make use of conducting plastic (PET) substrates. The techniques which need post-heat treatment for formation of desired films are difficult to implement as heat treatment consumes more time and may cause strain in the films. Therefore, it is desired and necessary to obtain a film at room temperature in single step without post-heat treatments.

In the present work, therefore, a special attempt has been made to deposit NiO thin films by cathodic electrodeposition onto FTO coated glass substrates at room temperature without post-heat treatments. The films thus prepared are subjected to their structural, morphological, optical and electrochromic characterizations. The successful demonstration of room temperature electrosynthesis of NiO samples would pave the way to fabricate flexible EC devices on PET substrates. This work is underway.

2. Experimental

NiO thin films were deposited from an aqueous nickel chloride bath containing 0.5 M nickel chloride (LOBA CHEMIE Extra Pure 97%) and 0.1 M KCl. The bath solution

* Corresponding author. Tel.: +91 231 2609230; fax: +91 231 2691533.
E-mail address: psp_phy@unishivaji.ac.in (P.S. Patil).

0925-8388/$ – see front matter © 2009 Elsevier B.V. All rights reserved.
doi:10.1016/j.jallcom.2009.09.146

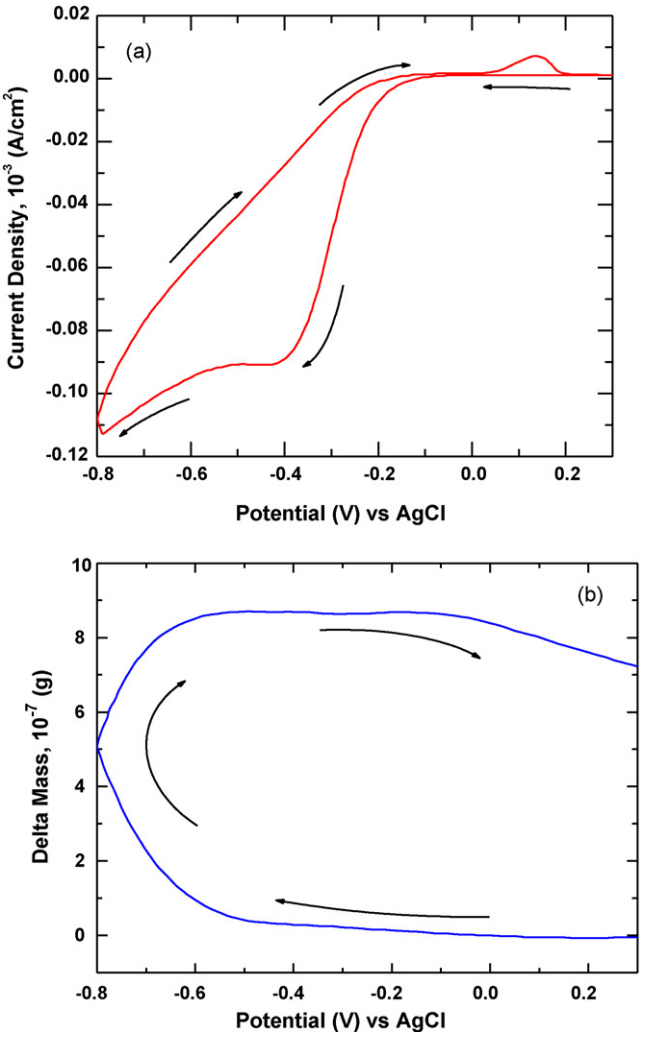

Fig. 1. (a) The reduction–oxidation behaviour of the electrolyte on the Pt electrode (area 1 cm^2) accompanied by (b) a concurrent shift in the delta mass of the quartz crystal electrode with the applied voltage.

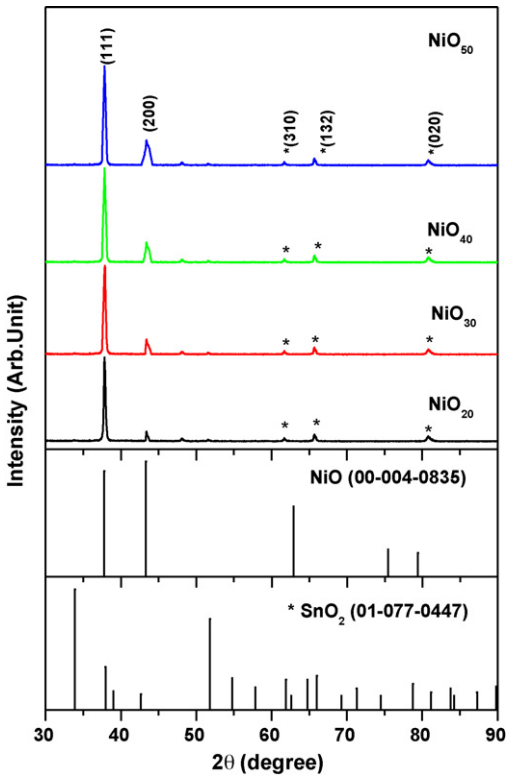

Fig. 2. X-ray diffraction patterns for NiO samples of different thicknesses where asterisk indicates the peaks of FTO (JCPDS file 01-077-0447). NiO peaks are indicated as (1 1 1) and (2 0 0) using JCPDS file (4-0835).

was complexed using EDTA (A.R. 99%) and pH was adjusted to 8 by addition of appropriate amount of KOH.

The conducting substrates used for deposition of NiO films in this study were FTO coated glasses having sheet resistance of 15–20 Ω/□. The graphite rod and Ag/AgCl respectively served as counter electrode and reference electrode. The NiO thin films were deposited at room temperature for different deposition times such as 20, 30, 40 and 50 min under potentiostatic condition resulting in different film thicknesses and are denoted by NiO_{20}, NiO_{30}, NiO_{40} and NiO_{50} respectively. Thickness of the film was measured using surface profiler (XP-1).

The structural and morphological characterization were carried out using a Philips-PW 3710 X-ray diffractometer with CuKα radiation (wavelength 1.5432 Å) and scanning electron microscopy (SEM) JEOL JSM-6360 respectively. The optical absorption and transmittance spectra of the samples in the coloured and bleached states were recorded using UV–vis–NIR spectrophotometer (Systronics—model 119) in the wavelength range of 350–850 nm. The powder collected from the deposited film was characterized by FTIR spectroscopy using Perkin Elmer IR spectrometer model-783 in the spectral range of 400–4000 cm^{-1}. To record IR patterns the pellet was prepared by mixing KBr with NiO powder (collected from thin film on glass substrate) in the ratio 300:1 and then pressing the powder between two pieces of polished steel. The electrochromic (EC) cell was again a standard three electrode electrochemical cell of configuration.

Glass/FTO/NiO/0.1 M KOH/C/Ag/AgCl

The NiO thin film deposited onto the conducting FTO (sheet resistance 15–20 Ω/□) coated glass substrate was used as working electrode. The counter electrode was a graphite rod and Ag/AgCl was used as a reference electrode. The electrolyte used was 0.1 M KOH solution. The cyclic voltammetry (CV), chronoamperometry (CA) studies were carried out using a VersaStat-II (EG & G) potentiostat/galvanostat, controlled by M270 software. All the potentials were measured with respect to Ag/AgCl. The EQCM were taken using an electrochemical analyzer (model CHI-400A) made by CH Instrument, USA. The EQCM measurements were performed on a platinum electrode coated on quartz crystal of 1 cm^2 area in a specially designed electrochemical cell with an aqueous 0.5 M $NiCl_2$ solution.

3. Results and discussion

To electrodeposit the NiO samples in one step initial investigations were made with the help of cyclic voltammetry and EQCM techniques. Following three electrode configuration was used: G/FTO/$NiCl_2 \cdot 6H_2O$ + EDTA + KOH + KCl/Pt.

The cyclic voltammogram was recorded in the range from +0.3 to −0.8 V versus Ag/AgCl in a 0.5 M nickel chloride solution at 10 mV/s. Fig. 1(a) and (b) is associated with the reduction–oxidation

Table 1
Various parameters of NiO films prepared at different thicknesses.

Time of deposition (min)	Thickness of the film (nm)	Band gap energy (E_g) (eV)	t_b (s)	t_c (s)	ΔOD	Colouration efficiency (cm^2/C)
20	104	3.2	2	1.7	0.71	107
30	154	3.1	2	2	0.59	45
40	542	3.1	2	3	0.50	25
50	615	3.0	3	3.2	0.46	15

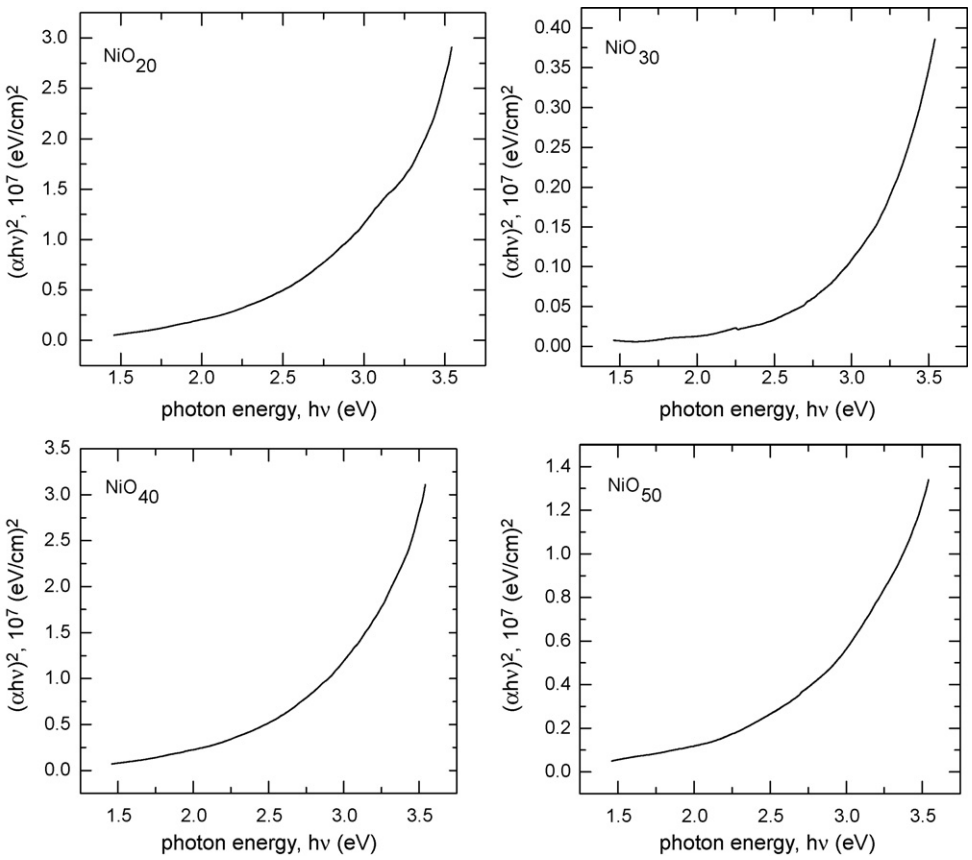

Fig. 3. Plot of $(\alpha h\nu)^2$ versus $(h\nu)$ for the NiO samples with different thicknesses.

behaviour of nickel species on the Pt electrode (area 1 cm^2) accompanied by a concurrent shift in the frequency of the quartz crystal electrode with the applied voltage. The arrows show the scan direction. The scans were initiated at +0.3 V versus Ag/AgCl, reversed at −0.8 V (versus Ag/AgCl) and terminated at +0.3 V (versus Ag/AgCl). During the cathodic scan, the increment in current density beyond −0.2 V (versus Ag/AgCl) is due to reduction of Ni^{2+} ions, where slight increase in mass takes place (Fig. 1(b)). The peak at −0.4 V is due to oxygen reduction [30–32]. The rapid increase in mass is observed beyond −0.5 V (Fig. 1(b)). According to EQCM theory [33–35] the shift in frequency is proportional to an increase of mass on the electrode surface according to Eq. (1):

$$\Delta f = \frac{-2f_0^2}{A\sqrt{\rho_q \mu_q}}\Delta m \quad (1)$$

where f_0 is the resonant frequency (Hz), Δf is the frequency change (Hz), Δm is the mass change (g), ρ_q is the density of quartz ($\rho_q = 2.648\ g\ cm^{-3}$) and μ_q is the shear modulus of quartz ($\mu_q = 2.947 \times 10^{11}\ g\ cm^{-1}\ s^{-2}$). The above relationship shows that an increase in mass leads to a decrease in frequency, and that the magnitude of the change in frequency is directly proportional to the mass change.

During the cathodic scan increment in current density starts at −0.2 V (Fig. 1(a)) due to reduction of Ni^{2+}, which is the onset of increase in mass onto the electrode (Fig. 1(b)). A peak at −0.4 V is due to a reduction of oxygen in the solution (Fig. 1(a)). This causes local pH to increase and a dip at −0.5 V on the *I–V* curve. The exponential increase in current density beyond −0.5 V is due to Ni $(OH)_2$ reduction (Fig. 1(a)) [18]. Subsequently, NiO growth takes place via intermediate steps of hydroxide formation given in Eqs. (2) and (3):

$$NiCl_2{\cdot}6H_2O + H_2O \rightarrow Ni(OH)_2 + 2HCl + 5H_2O \quad (2)$$

$$Ni(OH)_2 \rightarrow NiO + H_2O \quad (3)$$

The onset of deposition at −0.5 V (versus Ag/AgCl) followed by rapid rise in mass due to the growth of NiO and elemental Ni (Fig. 1(b)). Upon reversal of the plot scan, the mass deposited onto the electrode continues to increase up to −0.5 V and levelled off till 0 V (versus Ag/AgCl) (Fig. 1(b)). The slight decrease in the mass is due to stripping of elemental Ni between +0.1 and +0.2 V. This ensures pure NiO phase formation devoid of elemental Ni. Further, NiO films were deposited at various deposition times. The thickness of deposited NiO films with various deposition times is depicted in

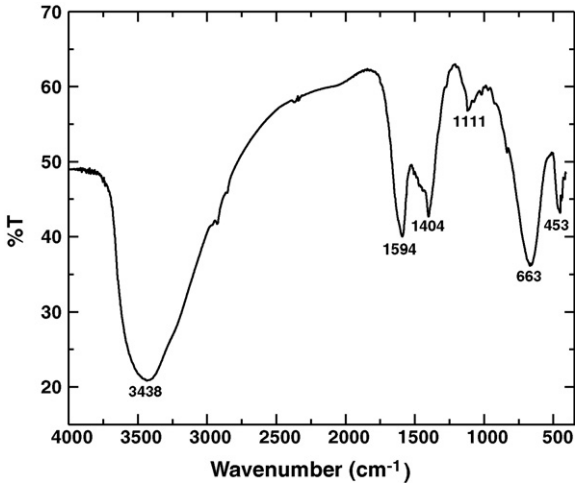

Fig. 4. FTIR spectrum for NiO_{30} sample recorded in the wavenumber of 400–4000 cm^{-1}.

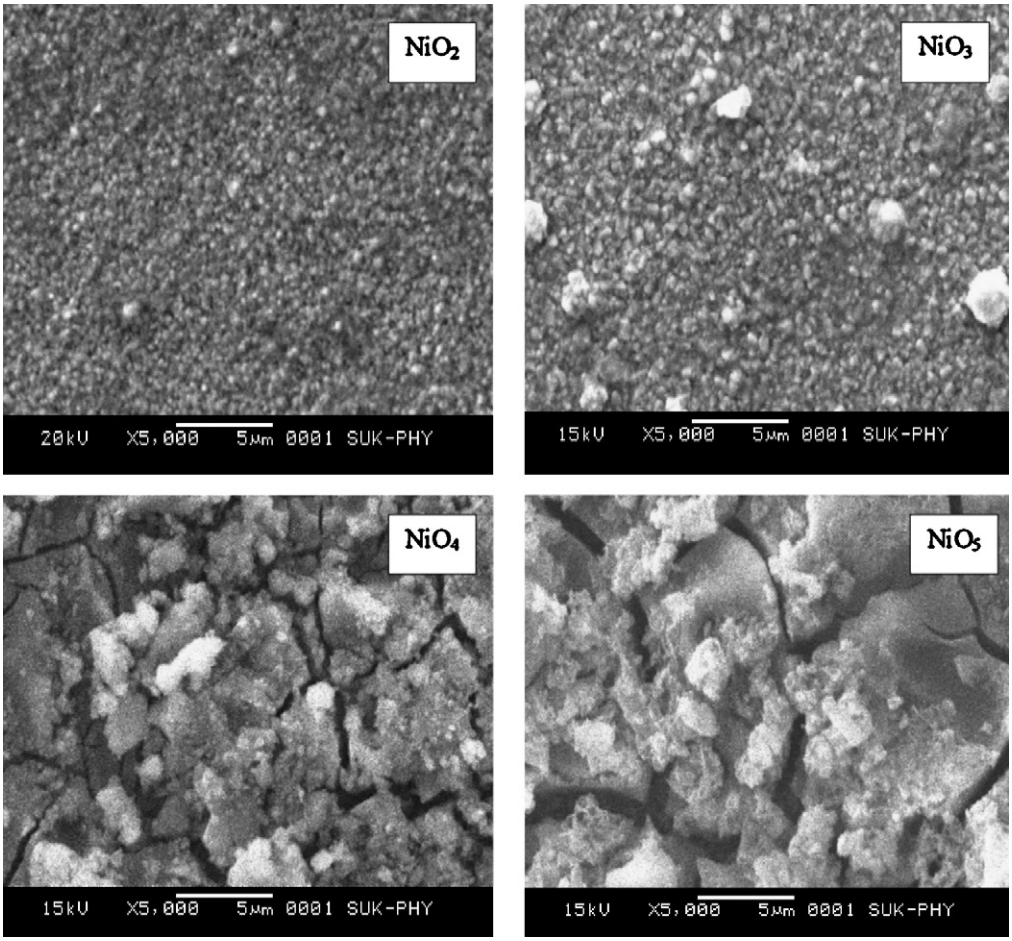

Fig. 5. Scanning electron microscopy (SEM) for all the samples deposited onto FTO coated conducting glass substrates. All the films are recorded at 5000× magnifications.

Table 1. Film thickness increases from 104 to 615 nm with increase in deposition time.

Fig. 2 shows X-ray diffraction (XRD) patterns of as-deposited nickel oxide thin films. Formation of polycrystalline NiO in cubic phase is confirmed (JCPDS file 4-835). The observed *d*-values and corresponding (*h k l*) planes are in good agreement. The similar results were reported by others [8,36,37]. The FTO substrate peaks were denoted by star (*) (JCPDS data file 77-0447). The presence of two XRD peaks along (1 1 1) and (2 0 0) planes in all the films suggests that the NiO phase is quite stable and its formation is independent of the film thickness. The crystallinity improves with increase in film thickness of NiO films, indicated by slight enhancement in peak's intensity. A slight improvement in crystallinity of the films with increase in film thickness is due to the ability of adatoms to move towards stable sites in the lattice, thereby favouring grain growth with preferred orientation [38].

The optical absorption data in the range of 350–850 nm was analyzed using a classical relation for near edge optical absorption in semiconductor [39]. Fig. 3 indicates a plot of $(\alpha h\nu)^2$ against $(h\nu)$ implies a direct band gap with an average value of 3.2 eV which agrees with reported values. The decrease in band gap energy with increase in film thickness is attributed to increase in crystallinity with film thickness [40]. The values are given in Table 1.

Fig. 4 shows the FTIR spectrum for NiO_{30} in the range of 400–4000 cm^{-1}. It shows the presence of six intensive bands at 3438, 1594, 1404, 1111, 663 and 453 cm^{-1}. A broad OH stretching band of hydrogen bonded water is seen at 3438 cm^{-1}. A water bending vibration is produced at 1594 cm^{-1}. The stretching vibration at 453 cm^{-1} can be assigned to nickel–oxygen interaction [41], while the vibration at 663 cm^{-1} belongs to the formation of hydroxide phase [42]. The existence of other bands clearly indicates that the sample consists of chloride ions, water molecules and/or hydroxide ions. IR study shows that water may initially present in the pores of NiO films or it may diffuse into the films from the electrolyte.

Fig. 5 shows scanning electron microscopy (SEM) images of as-deposited NiO thin films. A uniform granular and porous mor-

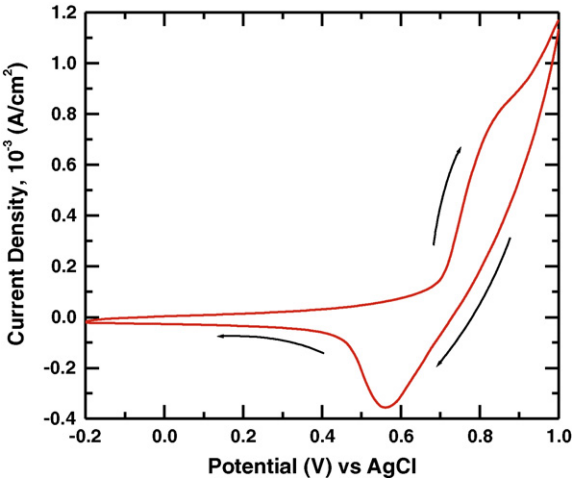

Fig. 6. Cyclic voltammogram recorded in 0.1 M KOH electrolyte for NiO_{30} sample The potential is swept from +1 to −0.2 V (versus Ag/AgCl) for NiO at the scan rate of 10 mV/s.

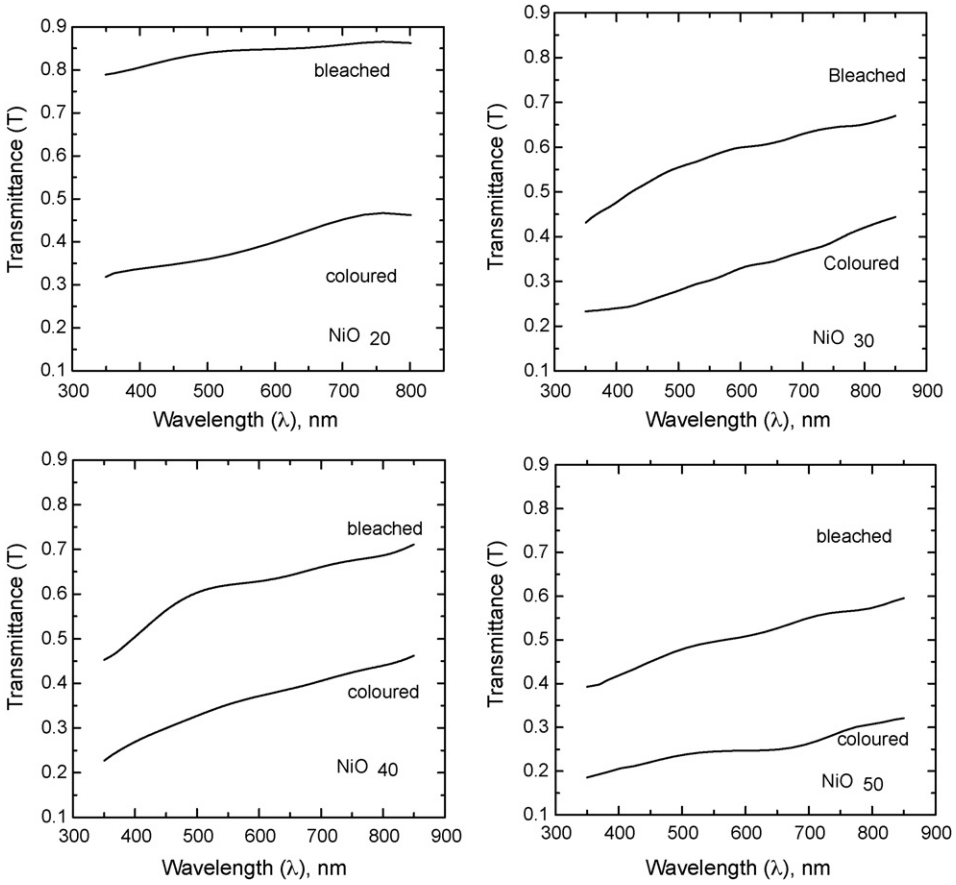

Fig. 7. Optical transmittance in coloured and bleached state recorded for all the samples. Optical transmittance c/b at various potentials versus Ag/AgCl in 0.1 M KOH electrolyte for all the samples of NiO recorded in the wavelength range 350–850 nm.

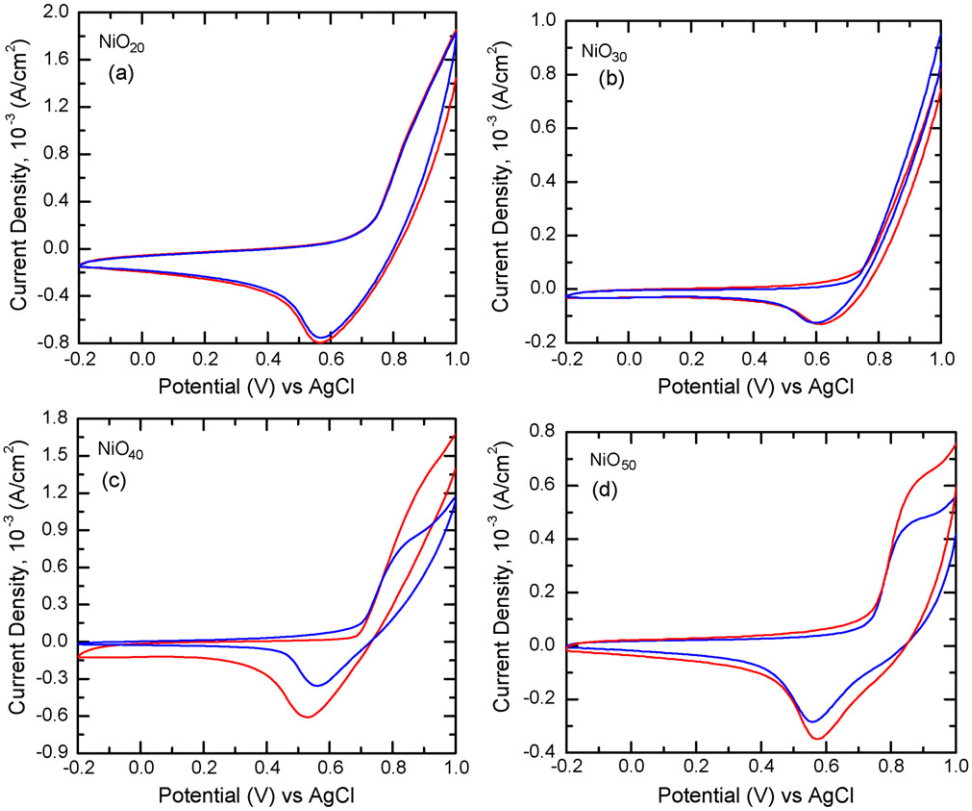

Fig. 8. Overlay of cyclic voltammograms for all the samples of NiO after 5th and 10,000th c/b cycle in 0.1 M KOH electrolyte demonstrating the electrochemical stability of the films at a scan rate of 20 mV/s.

phology of the films deposited for 20 min (NiO_{20}) was observed. The film becomes more compact and devoid of pores when deposition time was increased to 30 min (NiO_{30}). Thereafter severe cracks are observed for NiO_{40} and NiO_{50} samples. The cracked nature of the thicker films is attributed to the drying contraction caused due to tensile stress. It is reported that films with thickness greater that 0.2 μm are prone to cracking [43]. Similar results are also observed in cathodically deposited zirconia thin films [44] and galvanostatically deposited molybdenum oxide thin films [45].

A simplified reduction scheme for representing the gradual optical change that takes place under ion intercalation/deintercalation in electrochromic NiO films represented in Eq. (4):

$$\underset{\text{transparent}}{NiO} + xOH^- \Leftrightarrow \underset{\text{coloured (brownish gray)}}{NiOOH} + xe^- \quad (4)$$

The transition from NiO to NiOOH after intercalation and deintercalation of OH^- ions causes charge transfer from Ni^{2+} to Ni^{3+}. Due to charge transfer from Ni^{2+} to Ni^{3+}, films get coloured (brownish gray). Fig. 6 shows CV recorded for the sample NiO_{30} in potential window −0.2 to 1 V (versus Ag/AgCl) at the scan rate of 10 mV/s. Arrows indicate the scan direction. Electrochromism in NiO thin films is related to a charge-transfer process between Ni (II) and Ni (III) [21]. During the cathodic scan, the reduction of Ni^{3+} to Ni^{2+} leads to bleaching of the film (cathodic peak at 0.56 V). In the reverse anodic scan the oxidation of Ni^{2+} to Ni^{3+} causes colouration of the film (anodic peak at 0.76 V).

From CA studies, response time for all the four samples was determined. Response time for colouration (t_c) and bleaching (t_b) is the time required for the anodic/cathodic current to achieve a steady state level after the application of reactive voltages. CAs (not shown) were recorded for a potential step of ±0.7 V and the values of t_c and t_b estimated for all the samples are given in Table 1. It is observed that colouration time (t_c) increases with increase in film thickness while there is no appreciable effect on bleaching time (t_b).

The transmittance spectra of the samples in the coloured and bleached states were recorded in the wavelength range of 350 to 850 nm. Transmittance of the film decreases as the film thickness increases expectedly. Colouration and bleaching processes were carried out at ±0.7 V (versus Ag/AgCl) for a time step of 10 s. The optical data is normalized using FTO coated conducting glass substrate as reference while measuring the transmittance. The optical transmittance spectra of all the samples in their coloured and bleached states are shown in Fig. 7. The data is further used to calculate the colouration efficiency (CE) using the equation [46] as

$$CE_{\lambda=630\,nm} = \frac{(\Delta OD)_{630\,nm}}{Q_i} \quad (5)$$

where (ΔOD) is the change in optical density at λ = 630 nm and Q_i is the intercalated charge (mC/cm^2).

The electrochromic parameters for all the samples are given in Table 1. The value of CE is found to be maximum 107 cm^2/C for the sample NiO_{20}, which is high compared to the values reported in the literature by cathodically and anodically deposited NiO thin films [47–50]. Films with small grain sizes exhibit high CE supports the idea that large inner surface area of the film is connected to the electrochromic activity. Moreover its porous structure helps easier diffusion of ions and provides larger surface area for charge-transfer reactions. The improvement in the electrochromic activity of porous inorganic oxides has been reported in the literature [51–53].

The electrochemical stability of the film is one of the key parameters to be taken into account when one looks for its applications. Therefore, the film is further tested for long time electrochemical cycling and found to be stable above 10^4 colour/bleach (c/b) cycles. Fig. 8 shows the stability curves for all the films recorded at a scan rate of 20 mV/s. From the stability measurements it is observed that NiO_{20} films are more stable than other NiO films.

4. Conclusions

The feasibility of cathodic electrodeposition of electrochromic nickel oxide thin films at room temperature without post-heat treatment is confirmed. The reduction–oxidation behaviour of the electrolyte on the Pt electrode (area 1 cm^2) accompanied by a concurrent shift in the delta mass of the quartz crystal electrode with the applied voltage was studied which reveals the deposition of NiO on the substrate. X-ray diffraction analysis showed that as-deposited material is polycrystalline cubic NiO. Optical absorption study gives an average direct band gap of 3.2 eV. A uniform granular and porous morphology of the films deposited for 20 min was observed. The film becomes more compact and devoid of pores when deposition time was increased to 30 min. Thereafter severe cracks are observed. Maximum CE of 107 cm^2/C was observed for NiO_{20} film and is stable for 10^4 cycles, which can be attributed to the formation of favourable porous microstructure that facilitates easier diffusion of ions and provides larger surface area for charge-transfer reactions.

Acknowledgements

The authors wish to acknowledge the U.G.C., New Delhi for the financial support through the UGC-DRS II-phase and ASIST programme, and DST through FIST programme.

References

[1] E.J.M. O'Sullivan, E.J. Calvo, in: R.G. Compton (Ed.), Compr. Chem. Kinet. 27 (1987) 274.
[2] The electrochemistry of novel materials, in: S. Trasatti, J. Lipkowski, P.N. Ross (Eds.), Transition Metal Oxides: Versatile Materials for Electrocatalysis, VCH Publishers, New York, 1994, p. 207.
[3] C.M. Lambert, G. Nazri, P.C. Yu, Sol. Energy Mater. 16 (1987) 1–86.
[4] N. Shaigan, D.G. Ivey, W. Chen, J. Electrochem. Soc. 155 (4) (2008) D278–D284.
[5] E. Avendano, L. Berggren, G.A. Niklasson, C.G. Granqvist, Thin Solid Films 496 (2006) 30–36.
[6] M. Chigane, M. Ishikawa, Electrochim. Acta 42 (1997) 1515–1519.
[7] L.T. Kubota, Y. Gushikem, J. Electroanal. Chem. 3 (62) (1993) 219–225.
[8] K.K. Purushothaman, G. Muralidharan, J. Sol–Gel Sci. Technol. 46 (2008) 190–194.
[9] R. Cerc Korosec, P. Bukovec, B. Pihlar, A. Surca Vuk, B. Orel, G. Drazic, Solid State Ionics 165 (2003) 191–200.
[10] B. Sasi, K.G. Gopalchandran, Nanotechnology 18 (2007) 115613–115622.
[11] H. Kamel, E.K. Elmaghraby, S.A. Ali, K. Abdel-Hady, Thin Solid Films 483 (2005) 330–339.
[12] R. Cerc Korosec, P. Bukovec, Acta Chim. Slov. 53 (2006) 136–147.
[13] Y. Abe, S.-H. Lee, E.O. Zayim, C.E. Tracy, J.R. Pitts, S.K. Deb, Electrochem. Solid State Lett. 9 (2006) G17–G19.
[14] K.D. Lee, W.C. Jung, J. Kor. Phys. Soc. 45 (2004) 447–454.
[15] C.R. Magaña, D.R. Acosta, A.I. Martiĩnez, J.M. Ortega, Solar Energy 80 (2006) 161–166.
[16] M.-S. Wu, Y.-A. Huang, C.-H. Yang, J. Electrochem. Soc. 155 (2008) A798–A805.
[17] K.-X. He, Q.-F. Wu, X.-G. Zhang, X.-L. Wang, J. Electrochem. Soc. 153 (2006) A1568–A1574.
[18] F. Vera, R. Schrebler, E. Muñoz, C. Suarez, P. Cury, H. Goĩmez, R. Coĩrdova, R.E. Marotti, E.A. Dalchiele, Thin Solid Films 490 (2005) 182–188.
[19] X. Hou, J. Williams, K.-L. Choy, Thin Solid Films 495 (2006) 262–265.
[20] D. Perednis, L.J. Gauckler, Solid State Ionics 166 (2004) 229–239.
[21] C.G. Granqvist, Handbook of Inorganic Electrochromic Materials, Elsevier, Amsterdam, 1995.
[22] K.S. Ahn, Y.C. Nah, Y.E. Sung, J. Appl. Phys. 92 (2002) 7128–7132.
[23] M. Martini, G.E.S. Brito, M.C.A. Fantini, A.F. Craievich, A. Gorenstein, Elecrochim. Acta 46 (2001) 2275–2279.
[24] M. Gomez, A. Medina, W. Estrada, Sol. Energy Mater. Sol. Cells 64 (2000) 297–309.
[25] E. Avendano, A. Azens, G.A. Niklasson, C.G. Granqvist, Sol. Energy Mater. Sol. Cells 84 (2004) 337–350.
[26] A.I. Inamdar, S.H. Mujawar, V. Ganesan, P.S. Patil, Nanotechnology 19 (2008) 325706–325713.
[27] S. Morisaki, K. Kawakami, N. Baba, Jpn. J. Appl. Phys. 27 (1988) 314–318.
[28] D.A. Corrigan, R.M. Bendert, J. Electrochem. Soc. 136 (1989) 723–728.

[29] R.M. Bendert, D.A. Corrigan, J. Electrochem. Soc. 136 (1989) 1369–1374.
[30] L. Vaysiere, K. Keis, Hagfeldt, S.E. Lindquist, Chem. Mater. 13 (2001) 4395–4398.
[31] S. Peulon, D. Lincot, J. Electrochem. Soc. 145 (1998) 864–874.
[32] A. Goux, T. Pauporte, J. Chivot, D. Lincot, Electrochim. Acta 50 (2005) 2239–2248.
[33] A.W. Bott, Curr. Sep. Drug Dev. 18 (1999) 79–85.
[34] D.A. Buttry, M.D. Ward, Chem. Rev. 92 (1992) 1355–1379.
[35] G.Z. Sauerbrey, Z. Phys. 155 (1959) 206–222.
[36] D.A. Wruck, M. Rubin, J. Electrochem. Soc. 140 (1993) 1097–1104.
[37] Y. Sato, M. Ando, K. Murai, Solid State Ionics 113 (1998) 443–447.
[38] Y.H. Liu, L. Meng, L. Zhang, Thin Solid Films 479 (2005) 83–88.
[39] R.K. Kawar, P.S. Chirage, P.S. Patil, Appl. Surf. Sci. 206 (2003) 90–101.
[40] P.S. Patil, L.D. Kadam, Appl. Surf. Sci. 199 (2002) 211–221.
[41] S. Mochizuki, Phys. Stat. Sol. B 126 (1984) 105–114.
[42] A. Surca, B. Orel, B. Pihlar, J. Solid State Electrochem. 2 (1998) 38–49.
[43] I. Zhitomorsky, A. Petric, Mater. Lett. 46 (2000) 1–6.
[44] X. Pang, I. Zhitomorsky, M. Niewczas, Surf. Coat. Technol. 195 (2005) 138–146.
[45] R.S. Patil, M.D. Uplane, P.S. Patil, Appl. Surf. Sci. 252 (2006) 8050–8056.
[46] P.S. Patil, A.I. Inamdar, S.H. Mujawar, S.B. Sadale, Appl. Surf. Sci. 250 (2005) 117–123.
[47] C. Natarajan, S. Ohkubo, G. Nogami, Solid State Ionics 3 (1996) 949–953.
[48] M.M. Uplane, S.H. Mujawar, A.I. Inamdar, P.S. Shinde, A.C. Sonavane, P.S. Patil, Appl. Surf. Sci. 253 (2007) 9365–9371.
[49] YuZhenrui, SPIE 3560 (1998) 152–160.
[50] M.K. Carpenter, R.S. Conell, D.A. Corrigan, Sol. Energy Mater. 16 (1987) 333–346.
[51] X.H. Xia, J.P. Tu, J. Zhang, X.L. Wang, W.K. Zhang, H. Huang, Nanotechnology 19 (2008) 465701–465707.
[52] L.J. Chen, C.J. Lin, X. Cheng, Z.D. Feng, Solid State Ionics 148 (2002) 539–544.
[53] L. Dong, Y. Chu, W. Sun, Chem. A: Eur. J. 14 (2008) 5064–5072.